Heliyon 8 (2022) e11606

Contents lists available at ScienceDirect

Heliyon

journal homepage: www.cell.com/heliyon

Research article

White-flesh guava juice clarification by a fixed-angle conical rotor centrifuge laboratory and characterization of continuous disk stack centrifuges

Kombélé Aimé Ninga [a], Steve Carly Zangué Desobgo [b,*], Emmanuel Jong Nso [a], Joseph Kayem [a]

[a] Department of Process Engineering, National School of Agro-Industrial Sciences (ENSAI), University of Ngaoundere, P.O. Box 455, Adamaoua, Cameroon
[b] Department of Food Process & Quality Control, Bioprocess Laboratory, University Institute of Technology (UIT), University of Ngaoundere, P.O. Box 455, Adamaoua, Cameroon

A R T I C L E I N F O

Keywords:
Guava juice
Clarification
Efficiency
Lab centrifuge
Continuous centrifuge

A B S T R A C T

The two objectives of this paper were to determine the effect of centrifugation parameters on guava juice physicochemical characteristics and to identify operational characteristics of continuous disc-stack centrifuges based on the performance of a laboratory centrifuge. Effects of *g*-force (149 g–3731 g) and centrifugation time (10–40 min) on juice physicochemical characteristics (protein, pectin, galacturonic acid, dry matter, total soluble sugars contents; pH; electrical conductivity, clarity and particle size distribution) were assessed. Laboratory centrifuge performance was evaluated for 1343 g, 2388 g and 3731 g. At 1343 g, separation limits (x_{max}), feed flow-rates of disc-stack centrifuges and cut-off sizes (x_{50}) were determined for corresponding laboratory centrifuge operation times. Significant decrease in average particle size, protein and pectin contents was observed, contrary to juice clarity. Similar clarification efficiency was obtained for *g*-forces ≥ 1343 g. x_{max} were 2669 nm, 2200 nm and 1783 nm, with corresponding x_{50} for continuous centrifuges, 1887 nm, 1556 nm, 1261 nm, for 20 min, 30 min and 40 min, respectively.

1. Introduction

Guava (*Psidium guajava*) is a well-known tropical and sub-tropical fruit. Originated from USA, Columbia, Peru and Mexico, it is nowadays widely spread in different countries in Asia, Africa and South America (Ninga et al., 2021). Sometimes called "*superfruit*", it is well appreciated for its high vitamin A and C content (more than 4 times that of orange) (Surajbhan et al., 2012; Akesowan and Choonhahirun, 2013). Antioxidant capacity of its phenolic compound makes it suitable to trap free radicals in human body, therefore inhibiting formation and spreading of cancer cells (Flores et al., 2015). When stored at room temperature, guava fruit's shelf-life is 3–4 days, demonstrating its high perishability.

Due to its short shelf-life, guava can be processed into juice. Ninga et al. (2018) described kinetic models of hydrolysis of pectinaceous matter of guava pulp during depectinization. The effect of enzymatic treatment of guava pulp on the physicochemical parameters of the juice were described by Nso et al. (1998), Kaur et al. (2011), Le et al. (2012), Surajbhan et al. (2012), Akesowan and Choonhahirun (2013), Nguyen et al. (2013) and Marcelin et al. (2017). FESEM images were collected and analyzed, showing particles breakdown during depectinization of the pulp (Ninga et al., 2021).

After depectinization, some chemical interactions can take place in guava juice. Polyphenols and proteins can interact with haze or tannin formation. The former, because of their positive charge, will behave as a bridge and glue, thus implying the agglomeration of the latter (negatively charged). Tannin complexes could also be the result of polymerization of phenolic compounds into denser units (McLellan and Padilla-Zakour, 2005). There could also be some interactions between proteins and oligalacturonates from pectins hydrolysis (Shomer et al., 1999; Ninga et al., 2021). These interactions can lead to particles formation coupled with stone cells, affecting juice stability during storage (Wu et al., 2005).

Depectinized guava juice should be clarified to slow down haze formation during storage. Clarification is necessary to settle down the macromolecular particles (protein, polyphenol, cell wall, pectin and derived products) in fruit juice, to increase its acidity and to minimize the sucrose inversion level for longer shelf life (Ghosh et al., 2018). It can be done using filter-aids, centrifugation and microfiltration through membrane. Although some filter-aids such as chitosan may be non-toxic, the use of filter-aids requires the determination of suitable concentrations

* Corresponding author.
E-mail address: desobgo.zangue@gmail.com (S.C.Z. Desobgo).

https://doi.org/10.1016/j.heliyon.2022.e11606
Received 12 July 2022; Received in revised form 1 October 2022; Accepted 9 November 2022

and the combination of filtration to remove residues. Handling of these materials and the cost of waste disposal constitute a hurdle for the use of filter-aid (Sharma et al., 2015). Practical applications of membrane processes such as microfiltration face the major problem of reduction of the permeate flux due to irreversible fouling of membranes. Fouling occurs due to accumulation of pectin substances, tannins, proteins and fibers present in the juice on the membrane surface (known as concentration polarization) or blocking of the membrane pores (Rai and De, 2009; Sagu et al., 2014). Another unit operation for clarification of fruit juice is centrifugation during which particles will settle depending on their sedimentation velocity, thus forming a pellet at the sedimentation front and leaving clearer juice. Centrifugation describes less effect on the physicochemical and nutritional composition of the juice compared to microfiltration, since 4.6%–21.4% of polyphenols, and 19.9%–53.5% of proteins are removed during clarification compared to 28.6%–67.5% and 26.0–59.6% for polyphenol and proteins, respectively with microfiltration. Though producing more turbid juice due to less removal of suspended particles than microfiltration, centrifugation is proved to result in greater juice yield and is chemical free (Chhaya et al., 2013; Sagu et al., 2014; Biswas et al., 2016). Centrifugation of guava juice had been the subject of many research works. Kaur et al. (2009, 2011), Surajbhan et al. (2012), Marcelin et al. (2017) determined guava yield after centrifuging depectinized guava pulp at fixed rotation speed or *g*-force and centrifugation time. They also determined some physicochemical parameters of the juice without assessing the effect of processing conditions (*g*-force and time) on them. Moreover, clarification performance of different centrifuges used in those works was not assessed. Finally, the study of the dimensional and operational characteristics of a continuous centrifuge as a function of clarification performance of the guava juice of the laboratory centrifuge has not been done. This paper has two objectives: To determine the effect of *g*-force and centrifugation time on the physicochemical characteristics of clarified guava juice; and to identify operational characteristics of a continuous centrifuge from the clarification performance of a laboratory centrifuge.

2. Material and methods

2.1. Biological materials

Guava fruits (*Psidium guajava*) CV Lucknown 49, were purchased from local market in Kharagpur, West Bengal, India. Degree of maturity and ripeness were selection criteria.

Pectinase (Polygalacturonase) from *Aspergillus niger* (activity: 8000–12,000 U/g) was purchased from HiMedia laboratories Pvt. Ltd. (Mumbai, India).

2.2. Experimental set-up

The centrifuge used in this study was a refrigerated and programmable fixed-angle conical rotor laboratory centrifuge (Remi, R - 236M, Remi Elektrotechnik Ltd, West Bengal, India) (Figure 1A). It was equipped with a stainless-steel truncated conical bowl (rotor) model R - 236M (Figure 1B) with six tube accommodating holes. The tubes' inclination angle to the vertical axis was 20°. Geometric characteristics of the rotor are given in Table 1.

Table 1. Geometrical characteristics of the rotor R - 236 M.

Features	Minimum radius (mm)	Minimum study radius (mm)	Maximum radius (mm)	Average radius (mm)	Inclination angle to the vertical (°)
Values	≈30	≈54	133.5	≈82	20

2.3. Methods

2.3.1. Preparation of white guava juice for clarification

The extraction of guava juice was done following the procedure described by Ninga et al. (2021). Preliminary steps consisted of washing and rinsing of matured ripened guava fruits with tap water, followed by removal of blemishes by trimming, manual deseeding by a 16 – mesh sieve, blending using a food processor and mixing of the puree with demineralized water at a ratio of 35% w/w. The juice obtained underwent enzymatic treatment at 45 ± 2 °C under continuous stirring using a Remi Motor agitator, type RQ 122 (Elektrotechnik Ltd, Kolkata, India) at 1500 rpm. Operating conditions were: enzyme concentration = 0.078 weight of dried extract/weight of initial guava pulp; incubation time = 40 min. Enzyme preparation was inhibited by heat treatment of depectinized guava juice for 10 min at 95 ± 2 °C. The juice was cooled at room temperature, then filtered using a cheese cloth (200 μm mesh size). The filtrate was collected and kept in polyethylene terephthalate (PET) bottles, and stored in the freezer for further analysis.

2.3.2. Clarification of guava juice by centrifugation

Hundred grams of filtered guava juice were weighed at room temperature in 250 ml centrifuge tubes. Those tubes were introduced in the rotor of a laboratory centrifuge (Remi, R – 236M, Remi Elektronik Ltd, West Bengal, India). Centrifugation was done at 35 ± 3 °C. Centrifugation speeds used were 149 g (1000 rpm), 597 g (2000 rpm), 1343 g (3000 rpm), 2388 g (4000 rpm) and 3731 g (5000 rpm). Centrifugation times at constant speed were 10 min, 20 min, 30 min and 40 min. At the end of centrifugation, supernatant was collected in PET plastic bottles and kept in refrigerator for further analyses; whereas the pellets were discarded.

2.3.3. Determination of process parameters and physicochemical characteristics of guava juice

- Determination of the yield

The extraction yield of guava juice was determined using Eq. (1):

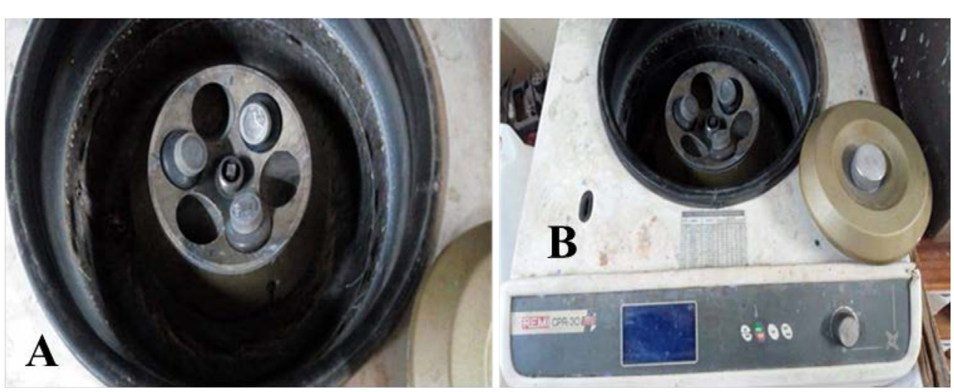

Figure 1. Image of the R - 236M rotor (A) and the laboratory fixed-angle conical rotor centrifuge (B).

$$\eta = \frac{m_s}{m_i} \times 100 \quad (1)$$

with η: the yield of guava juice (%); m_s and m_i weights of supernatant and initial guava juice (g), respectively.

- Particle size analysis of juice samples

The determination of the particle size of the supernatant was done at 25 °C using the Zetasizer based on the principle of dynamic light scattering (Malvern, Zetasizer nano, Malvern Instruments limited, UK). For this purpose, the dispersing medium used was demineralized water. For non-centrifuged guava juice, particle size distribution was obtained with the Mastersizer 2000 E (Version 5.20, Serial Number MAL1017204, Malvern Instruments Limited, United Kingdom). Average particle sizes were determined thanks to incorporated softwares. Particle size distribution curves of the centrifuged samples were fitted with Minitab 14 software using the log-normal model to determine the relationship between frequency (%) and particle size (nm) for each operating condition (*g*-force - centrifugation time) (Eq. (2)). An analysis of variance was performed to determine the significance levels of the parameters.

$$y = \frac{a}{x} \times e^{\left[-0.5\left(\frac{\ln\left(\frac{x}{x_0}\right)}{b}\right)^2\right]} \quad (2)$$

with x: particle size (nm); y: frequency (%). a and b are the model's constants, x_0 is the geometric average particle size.

For each operating condition, the parameters a, b and x_0 were estimated using Minitab 19.0 software and coefficients of determination were determined. The surface (%*nm) of each curve was determined by calculating the integral of log-normal models between two given particle sizes using Scientific Workplace version 5.5 software.

- Determination of Dry Matter Content

The determination of the dry matter content (DM) was done as follows. In a clean empty Petri dish (initial weight M_0), 5 g of guava juice was weighed and the total weight before drying (M_1) noted. The Petri dish was placed in an oven at 105 °C for 24 h. After drying, Petri dishes were removed and placed in a desiccator for cooling to room temperature. Final weight of the Petri dish (after drying) was determined (M_2). The dry matter content was determined using Eq. (3):

$$DM\ (\%) = \frac{M_2 - M_0}{M_1 - M_0} \times 100 \quad (3)$$

- Determination of other characteristics

Other physicochemical characteristics of the juice were determined. They represent quality attributes of juice and give more information on the nutritional value of the juice, its acidity and cloudiness. These characteristics were used to determine optimal conditions for centrifugation of guava juice and to determine the clarification performance of the laboratory centrifuge. These were: total soluble sugars (TSS), galacturonic acid, pectin, proteins contents; pH and electrical conductivity.

Protein content was determined using the method of Lowry; pectin content with the method using carbazole developed by McCready and McComb (1952) with some modifications as described by Ninga et al. (2021).

The clarity of guava juice samples was determined by measuring their transmittance at 660 nm using a UV-visible spectrophotometer (M/s Perkin Elmer, Connecticut, USA) against demineralized water as blank (Jain and De, 2016).

Total soluble sugars (TSS) were determined with a laboratory refractometer with digital display (Digital Lab Refractometer Salinity - 300034, Sper Scientific, Scottsdale, Arizona, United States of America) using demineralized water as blank (Ninga et al., 2021).

The galacturonic acid content was determined with the method using 2-cyanoacteamid with galacturonic acid as standard (Ninga et al., 2021).

pH and electrical conductivity were determined at room temperature with a pocket tester (Eutech Instruments Ltd, Singapore) by immersing electrodes in juice sample after calibration with demineralized water as described by Ninga et al. (2021).

For each characteristics, the ANOVA was done using Statgraphics Centurion software Version XV.II and 5 % significance level was utilized to check the difference between samples.

2.3.4. Determination of the dimensional and operational characteristics of continuous centrifuges

The objective was to determine the dimensional characteristics and feed flow-rate of a continuous centrifuge based on the performance of the laboratory centrifuge. Since the technological objective desired was centered on the supernatant (guava juice), centrifugal decanting was preferred over centrifugal dewatering (Towler and Sinnott, 2008; Koller, 2009). The bowl of the laboratory centrifuge used is a conical (truncated cone) type with a fixed angle (Figure 2A). The type of continuous centrifuge chosen in this study is the continuous disk stack-centrifuge. This choice was justified by the geometric similarity between the rotor of the laboratory centrifuge and a disc of the disk stack centrifuge (Figure 2B). This geometric similarity leads to a similarity in particle flow through the centrifuge tube and between two consecutive discs.

The determination of dimensional and operational characteristics of continuous disc stack-type centrifuges was done following the approach described by Maybury et al. (2000). They conducted a comparative study of the clarification performance of a laboratory centrifuge and a continuous disc stack centrifuge. The goal of this research was to develop a relationship between the clarification performance of laboratory centrifuge and that of continuous one. The study's purpose was to use the performance of a laboratory centrifuge to predict feed flow-rates of disc stack centrifuges.

- Determination of operating characteristics of the laboratory centrifuge

The determination of the clarification performance of the laboratory centrifuge required the determination of its sigma factor (Σ) or theoretical equivalent area using the equation described by Rayat et al. (2016). This represents the surface area of a gravity sedimentation tank capable of ensuring similar clarification performance to the centrifuge for the same suspension feed flow-rate (Svarovsky, 2000).

Considering the acceleration and deceleration times negligible compared to the operating time, the sigma factor of the conical rotor laboratory centrifuge was obtained from Eq. (4). This was generated by assuming the presence of a suspension consisting mainly of the cut-off size particle (x_{50}) with equal frequency in the supernatant and the pellet. For the calculation of this area, a laminar particle fall regime was assumed, thus neglecting mass transfer phenomena during centrifugation.

$$\sum_1 = \frac{V_1 \times \omega^2}{6 \times g \times \ln\left(\frac{2R_2}{R_1+R_2}\right)} = \frac{V_1 \times (2\pi N)^2}{3600 \times 6 \times g \times \ln\left(\frac{2R_2}{R_1+R_2}\right)} \quad (4)$$

with Σ_1: the sigma factor of the centrifuge (m^2); g: the acceleration of gravity ($m.s^{-2}$); ω: the angular velocity ($rad.s^{-1}$); N: the rotational speed (rpm); V_1: the volume of the feed (m^3); R_1 and R_2 minimum and maximum radial distances of sedimentation from the rotor axis (m).

The sigma factor was determined for the speeds 1343 g, 2388 g and 3731 g.

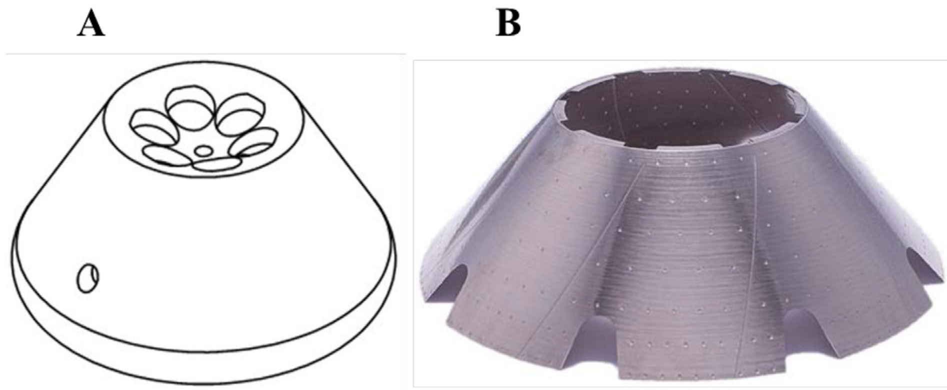

Figure 2. Three-dimensional representation of (A) the rotor of a laboratory fixed-angle conical rotor centrifuge and (B) a disc of a disc stack centrifuge (Alpha Laval).

- Determination of clarification performance of the laboratory centrifuge

This determination required that of the clarification efficiency (Eq. (5)) following the procedures described by Maybury et al. (2000) with some modifications. The optical density of each sample (feed and clarified samples) was determined at 660 nm using a UV-visible spectrophotometer (M/s Perkin Elmer. Connecticut. USA) against demineralized water as a blank. The centrifuged sample with the minimum optical density was used as the control.

$$CE\ (\%) = \left[1 - \left(\frac{OD_{\text{sample}} - OD_{\text{control}}}{OD_{\text{ali}} - OD_{\text{control}}}\right)\right] \times 100 \tag{5}$$

with: *CE*: the clarification efficiency (%); OD_{sample}, OD_{ali} and $OD_{control}$ optical densities of the sample feed and control sample, respectively.

For centrifugation speeds 1343 g, 2388 g and 3731 g, the clarification efficiency was plotted against separator capacity ($V_1/t/\lambda_{lab}\Sigma_{lab}$). V_1 is the volume of the processed sample (in m^3); λ_{lab} is the correction factor to characterize the deviation of the particle flow regime from the ideal regime in the case of the laboratory centrifuge. Σ_{lab} its theoretical equivalent area (in m^2) corresponding to the centrifugation speed, and *t* the centrifugation time (in s). For laboratory centrifuges, λ_{lab} is most often equated to 1 (Maybury et al., 2000; Boychyn et al., 2004). The optical density of the feed sample was equated to 2 with respect to the detection limit of the UV-visible spectrophotometer.

- Determination of maximum particle size (x_{max})

The centrifugation speed used for this purpose is 1343 g. This choice was guided by the significant variations of the parameters observed at this speed compared to the lower speeds and the negligible variations compared to the higher speeds (2388 g and 3731 g).

For that purpose, a preliminary determination of probability or *grade efficiency* of each particle to settle during centrifugation if the feed was exclusively made of it was done. Particle's frequency in distribution curves of both guava feed sample and clarified juice (for 20 min, 30 min and 40 min) were used as well as guava yield for each centrifugation condition using Eq. (6).

$$G_t(x) = 1 - (1 - E_{T_t}) \times \frac{dF_{f_t}(x)}{dF(x)} \tag{6}$$

with $G_t(x)$: the grade efficiency corresponding to the particle of size *x*; $dF_ft(x)$ and $dF(x)$: frequency of the particle of size x in the centrifuged and raw guava juice, respectively; E_{Tt}: the yield of guava juice centrifuged at 1343 g for a time *t* in min.

For the determination of x_{max}, grade efficiency was plotted against particle size. The particle size with the greatest grade efficiency closer to 1 was considered as the limit of separation.

- Determination of dimensional and operational characteristics of a continuous centrifuge for guava juice clarification

In case of linear correlation between clarification efficiency and separator capacity, equal performance of laboratory and disc-stack centrifuges could be predicted (Eq. (7)), thus enabling the determination of the feed flow-rate latter using its sigma factor and the separation capacity of laboratory centrifuge (Eq. (8)) as described by Maybury et al. (2000) and Rayat et al. (2016).

$$\frac{V_1}{t\sum_{lab}\lambda_{lab}} = \frac{Q}{\sum_{ds}\lambda_{ds}} \tag{7}$$

$$Q = \frac{V_1}{t\sum_{lab}\lambda_{lab}}\sum_{ds}\lambda_{ds} \tag{8}$$

with *Q*, Σ_{ds} and λ_{ds}, the feed flow-rate ($m^3.s^{-1}$), the sigma factor (m^2), and the correction factor for a deviation of the flow regime from the ideal regime of the continuous disk stack centrifuge. λ for disk stack centrifuges is equal to 0.4 (Maybury et al., 2000; Boychyn et al., 2004).

Intrinsic characteristics of a disc stack centrifuges found in literature (Table 2) were used to determine their sigma factor (Eq. (9)) for an equivalent *g*-force at 1343 g assuming that their volume flow rate is maximum (qV_{max}).

$$\sum = \frac{2}{3} \times \frac{\omega^2}{g} \times N \times \frac{\pi \times (r_2^3 - r_1^3)}{\tan\theta} \times F_L \tag{9}$$

with Σ: the sigma factor of the centrifuge (m^2); θ: inclination angle of discs from the vertical (°); *g*: the acceleration of gravity ($m.s^{-2}$); ω: the angular velocity ($rad.s^{-1}$); *N*: number of discs; F_L: the correction factor of caulks on discs; r_1 and r_2 inner and outer radii of the discs (m), respectively.

In case of available discs' specifications; F_L was determined using Eq. (10); otherwise; it was equated to 1.

$$F_L = 1 - \left(\frac{3Z_L B_L}{4\pi r_2}\right)\left(\frac{1 - \left(\frac{r_1}{r_2}\right)^2}{1 - \left(\frac{r_1}{r_2}\right)^3}\right) \tag{10}$$

with: Z_L the number of caulks on each disc; B_L: the height of a caulk (m).

Feed flow-rates of each centrifuge were determined at 1343 g for 20 min, 30 min and 40 min, respectively. The disk stack centrifuge with the greatest feed flow-rate of guava juice for a given operating time of the laboratory centrifuge was selected.

- Determination of the theoretical cut-off size (x_{50}) for the disc stack centrifuges

Table 2. Characteristics of commercial disc stack centrifuges identified in the literature.

Models	Manufacturers	r_{min}, r_{max} (mm)	N	Z	B (m)	θ (°)	Sources
Westfalia SAOOH	Westfalia Separator AG (Oelde. Germany)	21; 53	62	6	0.005	45	(Boychyn et al., 2004)
GEA OTC 2-03-107	Westfalia Separator Systems GmbH	22; 44	36		0.0025	40	(Cambiella et al., 2006)
SC6-06-076	Westfalia Separator (Oelde. Germany)	31; 62	76		0.0005	40	(Chlup et al., 2008)
Westfalia CSA-1	Westfalia Separator GmbH (Oelde. Germany)	26; 55	45			38.5	(Espuny, 2016)
Frau CN2S	Frau (Italy)	15; 54.5	51			52	(Jukkola et al., 2019)
Culturefuge 100™	Alfa Laval AB (Lund. Sweden)	36; 84.5	82	8	0.004	40	(Shekhawat et al., 2018)

Particle's theoretical grade efficiency or probability was plotted against its size for 20 min, 30 min and 40 min at 1343 g using Eq. (11), corresponding to disk stack centrifuges (Svarovsky, 2000). The cut-off size (x_{50}) is the particle size of probability 0.5. This particle size is independent of the initial suspension.

$$G(x) = \left(\frac{x}{x_{\max}}\right)^2 \tag{11}$$

with: $G(x)$: the probability corresponding to particles of size x (nm); x_{max}: the separation limits (nm).

3. Results and discussion

3.1. Effect of centrifugation parameters on the physicochemical characteristics of guava juice

3.1.1. Effect of centrifugation parameters on the extraction yield of guava juice

Centrifugation resulted in the guava juice at a yield between 89.72 ± 0.69 and 97.07 ± 0.69% w/w (Figure 3). The yield of juice extraction is almost 90% for all combinations of parameters applied. The juice yields obtained for 149 g are around 90% (91 ± 2% w/w). For *g*-forces between 597 g and 3731 g, extraction yields are greater than 95%.

An increase in *g*-force does not significantly affect the yield of guava juice, regardless of centrifugation times. The maximum percentage of pellets in the initial juice is approximately 2.5 ± 0.5%.

3.1.2. Effect of centrifugation parameters on the particle size distribution of clarified guava juice

The particle size distribution of the raw guava juice shows two peaks, the first around 2250 nm and the second around 90,000 nm (Figure 4). It appears that the particles with size between 22,440 nm and 251,785 nm are those with the highest proportion. They account for 72.77% of particles present in the feed sample. The average particle size is 72,138 nm. Particles greater than that represent 45.45% of all particles. It appears that non-centrifuged guava juice contains a broad range of large particles and aggregates which could either be those which passed through the filter cloth after enzymatic treatment or those resulting from interactions between deactivated proteins and oligogalacturonates from pectins hydrolysis (Shomer et al., 1999; McLellan and Padilla-Zakour, 2005).

For centrifuged guava juice samples, the distribution is of Fischer (Figure 5). For each centrifugal force, the increase in centrifugation time is accompanied by a progressive narrowing of the curves around the mean size. The smallest particle diameter is 68 nm for all each operating condition. The particle size distribution curve for the 149 g samples shows a predominance of particles with diameters between 615 nm and 1718 nm (Figure 5A). The decrease in the frequency of particles of a given diameter as a function of time for a given *g*-force would reflect a decrease in the number of these particles during centrifugation. The reduction in the width of the particle size spectrum with increasing centrifugation time for a given acceleration is accompanied by an increase in the proportion of finer particles.

Solid lines on each curve represent the fitting log-normal model. Model constants for different operating conditions were determined and reported (Table 3), as well as values of the coefficient of determination and analysis of variances.

These coefficients show an acceptable fitting of the log-normal model for particle size distribution curves. The surface areas of curves were obtained by calculating the integer of each model between 68 and 3091 nm and plotted for each operating condition (Figure 6).

Centrifugation has a remarkable effect for centrifugal accelerations of 597 g and 1343 g on the profile of the particle size distribution curves, whereas a quasi-linear trend was observed for 149 g, 2388 g and 3731 g (Figure 6).

For a given *g*-force, an increase in the centrifugation time led to a decrease in the width of particle size range as displayed in the surface vs particle size curve (Figure 6), therefore leading to a decrease in the average particle size of centrifuged guava juice samples (from 332 nm to

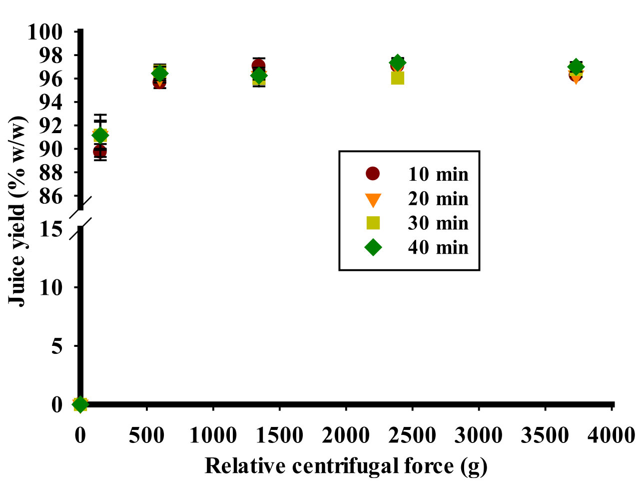

Figure 3. Yield of guava juice as a function of the relative centrifugal force applied.

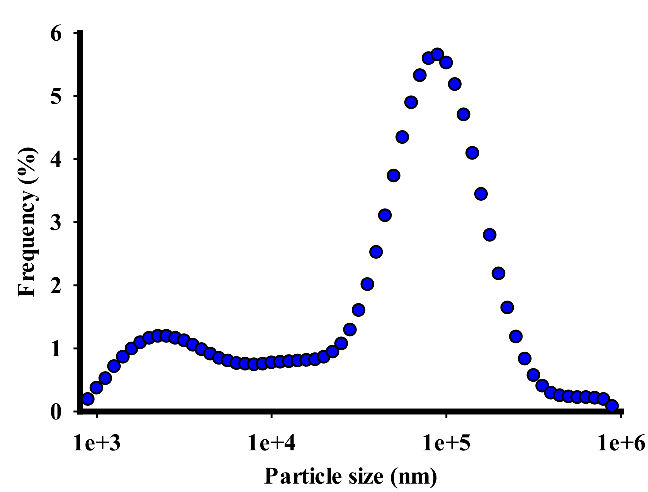

Figure 4. Particle size distribution of non-centrifuged guava juice.

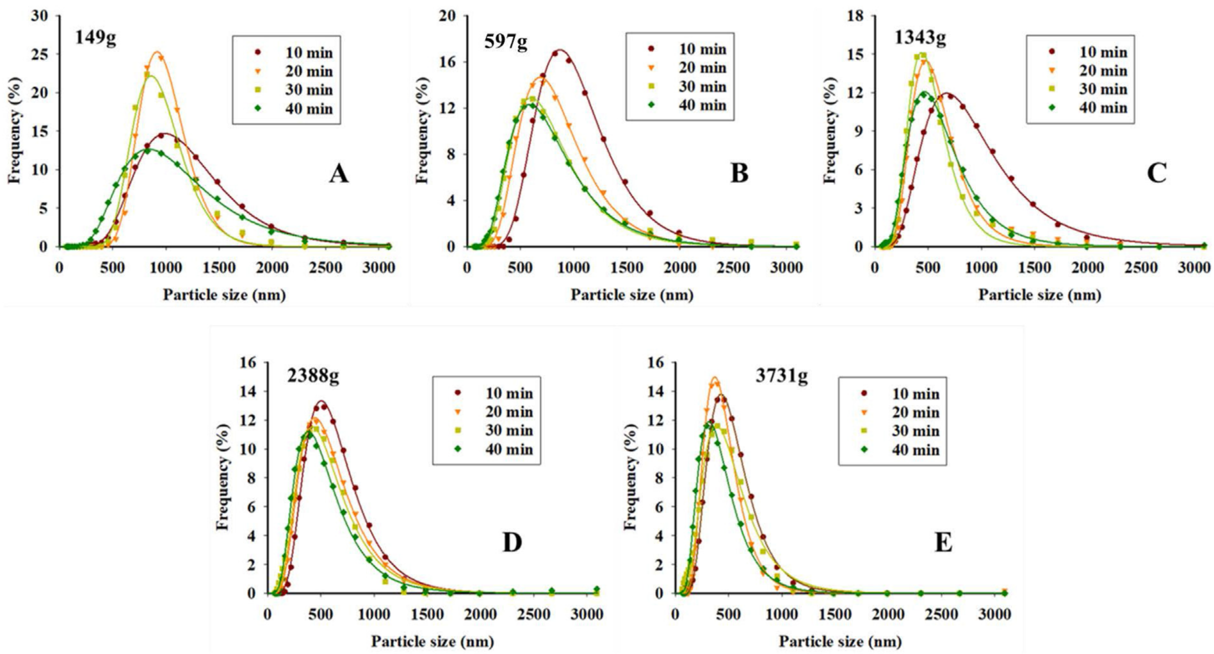

Figure 5. Particle size distribution of clarified guava juice. (A), (B), (C), (D) and (E) guava juices centrifuged at the indicated accelerations and centrifugation times.

1140 nm) (Figure 7). This could be explained by the fact during centrifugation, particles are submitted to centrifugal forces leading to their settling. According to Stokes' Law, the sedimentation velocity of a particle is a function of particle size, and the difference between the density of the particle and that of the fluid. The greater and denser the particle, the greater its sedimentation velocity. Particles would settle in the same magnitude of their sedimentation velocity, denser and larger particles settling first followed by lighter and smaller ones (Svarovsky, 2000). This led to a decrease in the average particle size observed in centrifuged sample, as the result of the narrowing of particle size distribution curves. The consequence is an increase in the clarity of guava juice as described further.

Increasing *g*-force while fixing the centrifugation time led to a decrease in the average particle size of centrifuged samples and their particle size ranges (Figures 6 and 7). This is in accordance to the result described by Chawafambira et al. (2015). The sedimentation velocity being a function of the centrifugal acceleration, increasing the *g*-force led to an increase in that velocity, thereby to the settling of particles in the same order of their velocity. Moreover, frictional forces acting on the particles and decreasing their sedimentation velocity would therefore be increasingly negligible compared to the centrifugal force (Robatel and Borel, 1989). An increase in *g*-force would lead to a progressive decrease in the effect of Brownian diffusion forces that act on fine particles, keeping them in suspension and opposing their sedimentation in the case

Table 3. Values of constants of the log-normal models, coefficients of determination and analysis of variances for each clarified guava juice sample.

Centrifugation parameters		Model Constants and Analysis of Variance Parameters					
g-force	Time (min)	a	b	x_0	R^2	Value of F	Probability (p)
149 g	10	15,631.2303	0.3732	1142.2940	0.9991	6884.3455	<0.0001
	20	23,822.1460	0.2298	966.6824	0.9984	3815.1160	<0.0001
	30	19,769.6168	0.2612	922.6080	0.9955	1324.8144	<0.0001
	40	11,801.2795	0.4658	1040.1947	0.9990	6295.6201	<0.0001
597 g	10	15,787.0226	0.3482	983.7673	0.9987	4668.9589	<0.0001
	20	10,913.1193	0.4006	806.1014	0.9980	2985.3766	<0.0001
	30	8533.0774	0.4463	731.5867	0.9976	2477.1187	<0.0001
	40	8068.4398	0.4746	733.1956	0.9996	16,730.3293	<0.0001
1343 g	10	9094.7421	0.4892	857.2055	0.9994	9681.9720	<0.0001
	20	7461.1000	0.3900	555.1124	0.9975	2348.0955	<0.0001
	30	7115.7952	0.3769	505.2511	0.9966	1734.6698	<0.0001
	40	6269.7107	0.4735	580.7774	0.9992	7287.9592	<0.0001
2388 g	10	7383.4772	0.4339	608.2819	0.9987	4756.9925	<0.0001
	20	6075.1861	0.4797	560.3254	0.9993	8461.0370	<0.0001
	30	5485.8938	0.4968	537.9501	0.9949	1156.6211	<0.0001
	40	4887.3994	0.5077	495.4160	0.9973	2195.9962	<0.0001
3731 g	10	6444.7337	0.4115	508.3661	0.9991	7024.2033	<0.0001
	20	5986.8620	0.3838	429.2792	0.9992	7350.1895	<0.0001
	30	5034.3938	0.4840	486.5226	0.9927	811.4094	<0.0001
	40	4235.7907	0.4733	397.8415	0.9973	2182.9271	<0.0001

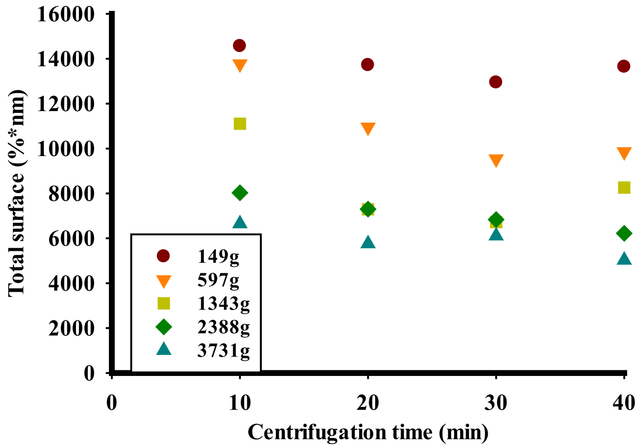

Figure 6. Particle size spectrum surface as a function of centrifugation parameters.

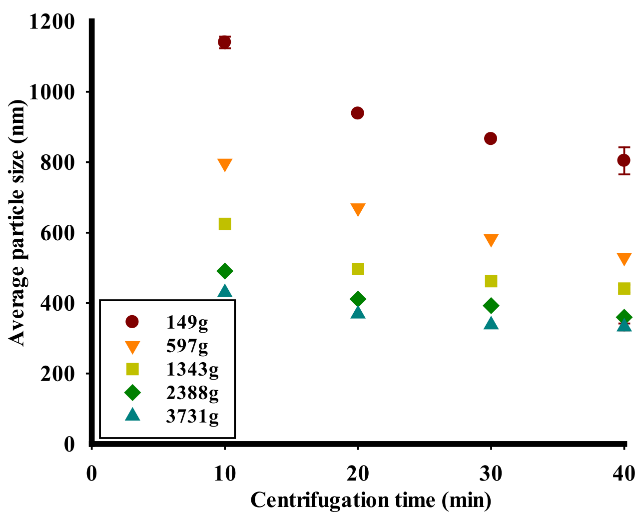

Figure 7. Average particle size of clarified juice as a function of centrifugation parameters.

of gravity sedimentation (Svarovsky, 2000). Resulting supernatants (juice) contained finer particles with decreasing maximum particle sizes as the *g*-force increased.

For *g*-force ranging from 1343 g to 3731 g, there was no significant effect of centrifugation on the average particle size for centrifugation times greater than 20 min (Figure 7). This is similar for the surface vs particle size curves. This could be explained by the fact that there could be no significant difference in the sedimentation velocity of particles for those clarification conditions.

3.1.3. Effect of centrifugation parameters on the clarity of guava juice

The clarity of the different guava juices ranged from 0 to 68.72 ± 2.18% Transmittance. That of the feed sample was not measurable by the spectrophotometer (Figure 8). The effect of time and centrifugal acceleration on clarity showed a trend opposite to that of average particle size. An increase in time or centrifugal acceleration is accompanied by an increase in clarity of banana juice as observed by Sagu et al. (2014). Ghosh et al. (2018) also highlighted an increase in clarity of the jamun juice with an increase in time and centrifugation speed. A maximum clarity of 83.60 %T was described by them with 60 min of centrifugation at 8000 rpm. Details of the rotor used by them being absent, *g*-forces corresponding to their rotation speeds could not be calculated, therefore a comparison could not be made between their work and this research work.

The increase in percentage transmittance during centrifugation could be due to the increase in scattered light intensity caused by the reduction in the particle size spectrum of the colloidal particles in guava juice. The clarity of guava juice would reflect the behavior of suspended particles and macromolecules of samples towards the incident light beam at 660 nm. Values of electrical conductivity revealed the presence of charges in the samples. When a light beam passes through the sample, it could be scattered by negatively charged particles of the juice due to the presence of electric field and a diffuse layer around them. Settling of particles based on their sedimentation velocity could result in an increase in the clarity. This results in the presence of smaller particles in greater proportion in the juice. The smallest hydrodynamic diameter measured in each sample is 68 nm, i.e. greater than 1/10 of measurement wavelength (660 nm) (Figure 5 B–E). The intensity of scattered light depends on the particle size. The larger the particle, the greater the intensity of the scattered light (Malvern Instruments, 2013). Settling of larger particles results in the presence of smaller one in clarified juice. That could result in an increase in the intensity of transmitted light coming out from the cuvette. The intensity of light scattered by particles depends on their size and number. The larger the particle, the greater the intensity of the scattered light (Malvern Instruments, 2013).

Guava juice samples corresponding to *g*-force 149 g and 597 g (10 min) contained large particles ($d > 660$ nm) that could cause complete scattering of light due to multiple light scattering, resulting in a 0 % Transmittance (Figure 8). For *g*-forces ranging from 1343 g to 3731 g, for $t > 10$ min, particles with diameter less than 660 nm accounted for 75% in each sample. Less light scattering could be observed in these samples, resulting in an increase in clarity with increasing time. The same phenomena could be observed for 597 g.

For 3731 g, a maximum clarity of 70 %Transmittance is obtained (Figure 8). Sagu et al. (2014) obtained similar results after centrifuging banana juice at 6000 g for 60 min, showing that more energy was consumed in their case. The increase in clarity between 30 and 40 min of centrifugation is not significant.

3.1.4. Effect of centrifugation parameters on the pectin content of guava juice

The pectin content of the non-centrifuged sample was 426.70 ± 34.54 mg/L. Centrifugation contributes to decrease the pectin content to a value between 238.69 and 19.23 mg/L (Figure 9). For each *g*-force, increasing the centrifugation time led to a decrease in pectin content of clarified juice. 85% of pectin content reduction was recorded for 1343 g, whereas 93 and 96% were depicted for 2388 g and 3731 g, respectively. That significant decrease was followed by an insignificant one, with slopes from 10 min to 40 min of 1.52%, 0.84% and 0.03% for 1343 g, 2388 g and 3731 g, respectively. For 149 g and 597 g, the decrease in

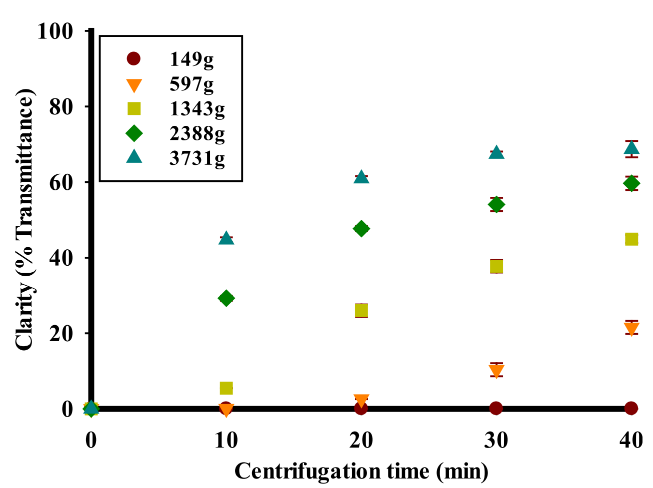

Figure 8. Clarity of guava juice as a function of centrifugation parameters.

pectin content is correlated with a decrease in the values of slopes between two consecutive time intervals.

The decrease in pectin content, just like that of average particle size, could mean that among the particles which settled during centrifugation could there be those made of pectins of pectinaceous matters. Oligogalcturonates resulting from pectins hydrolysis are negatively charged; they could therefore be subject to ionic interactions with positively charged compounds such as proteins, yielding in the formation of complex particles (Jaarsveld et al., 2005; Ninga et al., 2021). During centrifugation, these particles, depending on their size, sedimentation velocity and the clarification conditions, could settle forming the pellet. Particles in the supernatant could have a non-significant difference in affinity with ethanol solution used to precipitate pectins and pectinaceous matters during analysis. That could explain linear decreasing trends with small values of slopes observed between 10 and 40 min for 1343 g, 2388 g and 3731 g. This corroborated with the decrease in average particle size with respective slopes 10.74%, 7.65% and 5.65% for 1343 g, 2388 g and 3731 g (Figure 9). This could be supported by the progressive narrowing of the particle size distribution curves around 200 nm–1000 nm for all samples obtained using these centrifugal forces (Figure 5 C–E).

An increase in *g*-force was accompanied by a decrease in pectin content. This corroborates with results described by Sagu et al. (2014). When centrifuging depectinized banana juice, they observed a decrease in alcohol insoluble solids (AIS) (among which pectins) with an increase in acceleration.

3.1.5. Effect of centrifugation parameters on the protein content of guava juice

The protein content of non-centrifuged guava juice is 713.24 ± 23.87 mg/L. The protein content decreases over the clarification time for all centrifugal accelerations applied (Figure 10). For samples centrifuged at 1343 g, 2388 g, 3731 g, after 10 min of separation, more than 45% of protein content reduction could be observed. This was followed by insignificant decrease up to 40 min (slope 5.64% and 3.46%, respectively), as can be seen with error bars. In the case of centrifugal acceleration of 597 g, there is a decrease in protein content with a gradual decrease in the slope between two consecutive values of centrifugation time. This decrease is not considerable between 20 min and 40 min. For 149 g, the decrease in protein content after the first 10 min (21% of the value of the non-centrifuged guava juice) is followed by a moderate decrease (16.10% of the value at 10 min) between 10 and 40 min. Ghosh et al. (2018) described a decrease in protein content of jamun juice with an increase in time and centrifugation speed.

Protein content during centrifugation showed a similar trend to that of pectin content and particle size. Proteinaceous particles would be among those that settle during centrifugation. These particles could be the results of the complexation of protein molecules with other molecules, such as oligogalacturonates, polyphenols and chelating anions present in the milieu (Siebert, 1999).

The decrease in protein content with increasing *g*-forces was also recorded by Sagu et al. (2014) in case of banana juice with protein content decreasing from 1060 mg/L to 610 mg/L with acceleration increased from 2000 g to 10,000 g. They also reported that centrifugation had less effect on the juice protein content compared to microfiltration. Biswas et al. (2016) described similar results with bottle gourd. Juice obtained with centrifugation could have greater nutritional values compared to that obtained with microfiltration. A comparative study needs to be done in the case of guava.

3.1.6. Effect of centrifugation parameters on other physicochemical characteristics of guava juice

- Effect of centrifugation parameters on the total soluble sugars (TSS) and galacturonic acid content

The total soluble sugar content of the initial sample is 2.3 ± 0.0°Bx. Centrifugation results in an increase in the total soluble sugar content (Figure 11). The total soluble sugar content of centrifuged samples is greater than that of non-centrifuged one. However, the increase in time and centrifugal acceleration does not show a significant effect between different centrifuged samples. This corroborates with the results obtained by Ghosh et al. (2018) for jamun juice. They also obtained almost equal values of TSS both with centrifugation and microfiltration. Márquez-Montes et al. (2022) described an increase in TSS after cryocentrifugation of prickly pear juice. When clarifying guava juice with ultrafiltration using 100 kDa polyethersulfon membrane, Omar et al. (2020) observed a 7–17% decrease in TSS value compared to that of fresh juice. This was similar to the observations done by Ghosh et al. (2018) and Biswas et al. (2016) who obtained smaller values of TSS with microfiltration than that of centrifugation. This means that membrane processes could lead to a decrease in soluble sugars, therefore affecting the nutritional value of the juice. The biological and the microbial stabilities of the juice were not studied in the present work.

Centrifugation is not appropriate for separating soluble compounds from juice with a low molecular weight. This could also explain the insignificant effect of centrifugation parameters on the galacturonic acid content of guava juice (Figure 12).

- Effect of centrifugation parameters on dry matter content

The dry matter content of the initial sample is 2.85 ± 0.12% w/w. It appears that centrifugation contributes to a considerable decrease in the

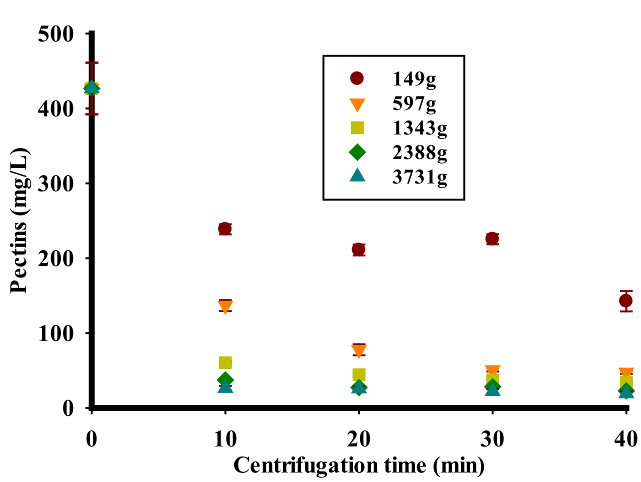

Figure 9. Pectin content of clarified guava juice as a function of centrifugation parameters.

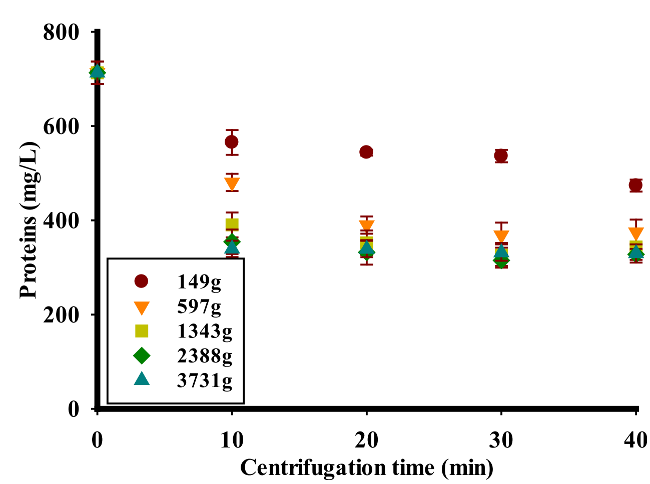

Figure 10. Protein content of clarified guava juice as a function of centrifugation parameters.

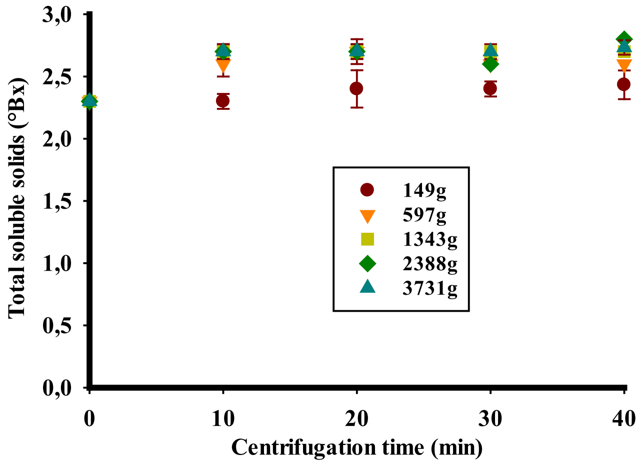

Figure 11. Total soluble sugar content of clarified juice as a function of centrifugation parameters.

dry matter content of guava juice compared to the non-centrifuged one (Figure 13). The significant decrease in dry matter content could be explained by particles sedimentation during centrifugation. Varying the centrifugation parameters does not significantly affect the dry matter content of the clarified samples (Figure 13).

- Effect of centrifugation parameters on pH value

The pH of the non-centrifuged guava juice is 3.71 ± 0.00. The pH does not vary significantly with increasing centrifugation parameters (Figure 14). Monomers and oligomers of galacturonic acid could display buffering behavior leading to an insignificant change in pH (Ninga et al., 2021). Ghosh et al. (2018) described an increase in pH value with an increase in centrifugation time; however, a decrease in pH values with an increase in centrifugation speed was recorded. Similar results were obtained for prickly pear juice by Márquez-Montes et al. (2022). Clarification of guava juice with ultrafiltration did lead to significant change in pH value as observed by Omar et al. (2020).

- Effect of centrifugation parameters on electrical conductivity

Centrifugation contributes to a decrease in the electrical conductivity of the clarified samples (Figure 15).

The electrical conductivity of the non-centrifuged guava juice is 1828.33 ± 7.51 mS/cm. Greater proportion of charged particles are present in non-centrifuged sample than in centrifuged ones with not-significant difference among them. Colloidal particles of the different samples would have electrical charges whose total does not lead to a considerable variation in conductivity regardless of the values of the clarification parameters. Conductivity of the samples is also the result of the charge of dissolved ions present in samples.

3.2. Determination of the dimensional and operational characteristics of a continuous disk stack centrifuge

3.2.1. Determination of the operating characteristics of the laboratory fixed-angle conical rotor centrifuge

Thanks to the geometrical characteristics given in Table 1, sigma factors of lab centrifuge rotor were calculated for 1343 g, 2388 g and 3731 g; these were 0.475 m^2, 0.844 m^2 and 1.318 m^2, respectively. An increase in the acceleration led to an increase in sigma factor, thus a greater sedimentation surface.

3.2.2. Determination of separation performance of the laboratory centrifuge

The clarification efficiency is an important factor in comparing the separation performance of the centrifuge for the different operating conditions. The performance of the centrifuge for different operating conditions is shown in Figure 16.

For all centrifugal accelerations, the clarification efficiency decreases with separator capacity (Figure 16). For the 1343 g acceleration, it decreases from 95% to 71% for separator capacities ranging from $8.77*10^{-8}$ $m.s^{-1}$ to $3.51*10^{-7}$ $m.s^{-1}$. For 2388 g and 3731 g, it decreases from 98.41% to 90. 35% and from 100% to 95.15% for capacities ranging from $4.94*10^{-8}$ $m.s^{-1}$ to $1.97*10^{-7}$ $m.s^{-1}$ and from $3.16*10^{-8}$ $m.s^{-1}$ to $1.26*10^{-7}$ $m.s^{-1}$, respectively. Separator capacity is the ratio of feed flow-rate per unit area of sedimentation. Clarification efficiency reflects the centrifuge performance under operating conditions. It describes the behavior of a gravity sedimentation tank with a specific sedimentation area, if it was fed with a given flow-rate of guava juice. The decrease in clarification efficiency as a function of separator capacity could be explained by the increase in the amount of settled solids with the decrease in feed flow-rate. The suspension feed flow-rate being small coupled with reduced effect of leaching, its residence time in the tank would be long resulting in an increase in the amount of settled solids (Koller, 2009). Moreover, an increase in *g*-force led to an increase in the clarification efficiency because of an increase in the corresponding surface area for sedimentation.

The increase of the *g*-force leads to a progressive narrowing of the scatter (Figure 16). For each acceleration, linear regression fitting was done with R^2 values being 99.70%, 99.90% and 99.80%, for 1343 g,

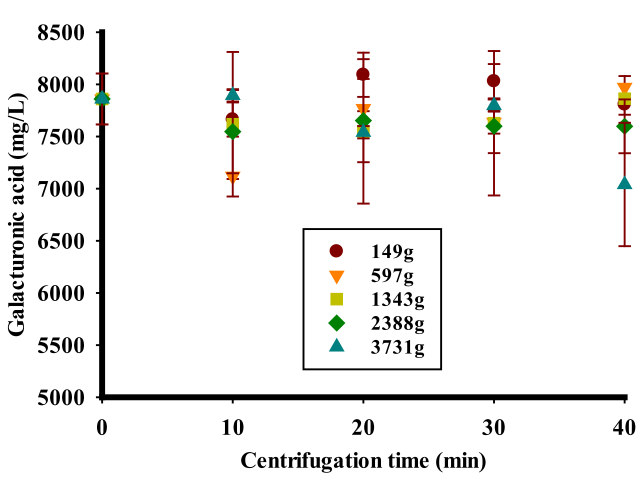

Figure 12. Galacturonic acid content of clarified juice as a function of centrifugation parameters.

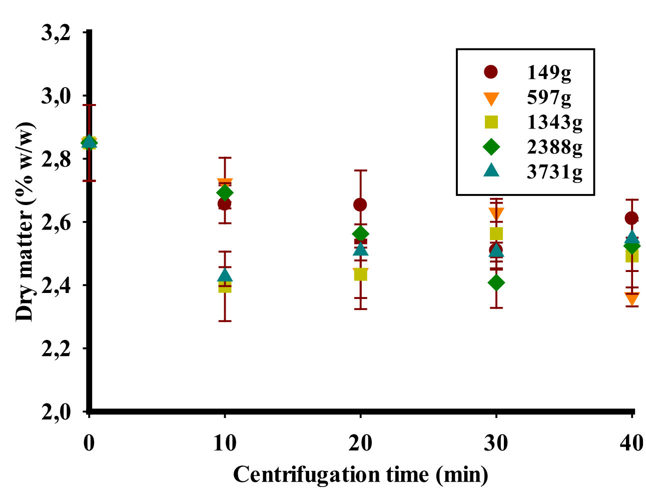

Figure 13. Dry matter content of clarified juice as a function of centrifugation parameters.

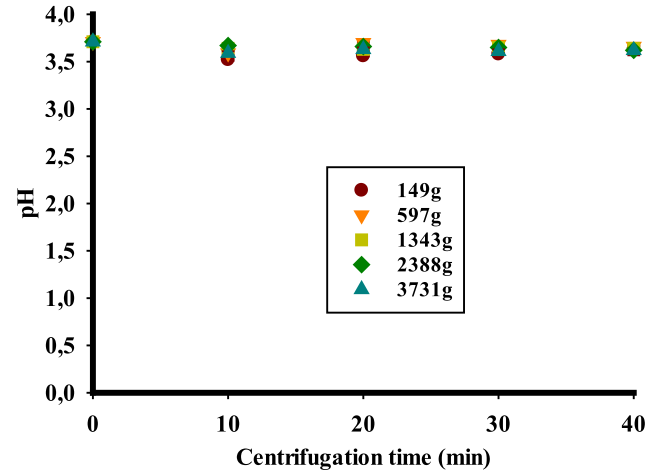

Figure 14. PH of clarified juice as a function of centrifugation parameters.

2388 g and 3731 g, respectively, with corresponding slopes $-9{,}20 \times 10^7$, $-5{,}39 \times 10^7$ and $-5{,}27 \times 10^7$. Decreasing absolute value of slopes with increasing *g*-forces could be related to the decrease in surfaces of particle size distribution curves (Figure 6). This is contrary to the results obtained by Boychyn et al. (2004), who explained greater absolute value of slope with narrowing of particle size distribution without showing the graph.

The linear correlation between clarification efficiency and separator capacity for each acceleration concluded that the performance of the laboratory centrifuge could be used to predict that of a continuous disc stack centrifuge with a given sigma factor (Maybury et al., 2000). The equation of regression line can be used to predict the feed flow-rate of that disc-stack centrifuge corresponding clarification efficiency.

Except the clarified juice sample at 1343 g for 10 min, a difference in clarification efficiency of less than 10% was obtained for all operating conditions bestowing a similar performance for 1343 g, 2388 g and 3731 g (Figure 16). This is in agreement with the results observed by Maybury et al. (2000). They reported a non-significant difference in clarification efficiency at 1312 g and 3870 g. Moreover, this non-significant difference was also observed for several physicochemical parameters obtained with these operating conditions. 1343 g was used as optimal *g*-force for further works.

3.2.3. Determination of maximum particle size (x_{max})

The grade efficiency varies from 0 to 1 for all centrifugation times (Figure 17). The particle size range varies from 68 nm to 3010 nm. Grade efficiency of particle less than 893 nm was assumed to be 0 due to limit of detection of the Mastersizer. Beyond 893 nm, grade efficiency increased with particle size for each centrifugation time. Depending on centrifugation conditions, there was a given particle size beyond which probability is equal to 1. It corresponds to the particle having the smallest probability to be detected in the supernatant if the feed was exclusively made of it. That is separation limit (x_{max}) and is 2669 nm, 2200 nm and 1783 nm, for 20 min, 30 min and 40 min respectively. It can be noticed that as separation time increased, limit of separation decreased. Particles bigger than the separation limit could easily be removed during centrifugation, since their probability is equal to 1 (Svarovsky, 2000).

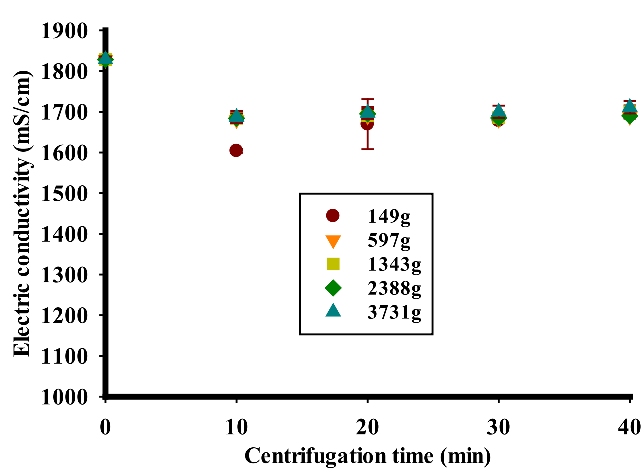

Figure 15. Electrical conductivity of clarified juice as a function of centrifugation parameters.

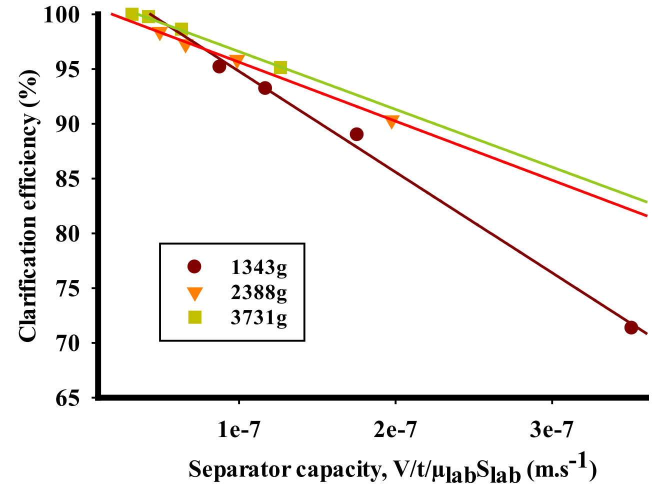

Figure 16. Performance of the laboratory centrifuge for 1343 g, 2388 g and 3731 g.

For particle diameters between 68 nm and 1262 nm, the probability increases steeply with the particle size (Figure 17). For that range, an insignificant increase (less than 100 nm) in the particle size led to a significant increase in the probability (probability difference greater than 0.1). It gives information on the sensitivity of centrifugation. This can be noticed in the particle size distribution curves, since two particles of size difference less than 100 nm were having frequency difference greater than 1% (Figure 5 C–E). During centrifugation, their sedimentation velocity can be significantly different with a rapid settling of the greater one.

Above 1262 nm, the probabilities increase non-significantly towards 1 (Figure 17). Thus, two particles with a particle size difference of 500 nm have equal probabilities of being removed by centrifugation. In addition, a negligible difference in probabilities is observed with increasing centrifugation times. This corroborates with the frequencies obtained for each particle diameter (Figure 5 C–E).

3.2.4. Determination of feed flow-rates for disc stack centrifuges of known dimensions

Sigma factors used are those corresponding to 1343 g. Table 4 shows feed flow-rates for disc stack centrifuges for each run time of the laboratory centrifuge.

For a given continuous centrifuge, increasing the run time of the laboratory centrifuge results in a decrease in its feed flow-rate to ensure similar performance to that of the latter (Table 4). Similarly, increasing the sigma factor results in an increase in the feed flow-rate for a given run time of the laboratory centrifuge.

For a given run time of the laboratory centrifuge, the Culturefuge 100™ model has the highest feed flow-rate. With neither centrifuge prices nor technical specifications available, the main criterion for selection was feed flow-rate. However, the choice of a disk stack centrifuge model will depend on the operator depending on the volume of sample to be processed and the corresponding feed flow-rate.

3.2.5. Determination of theoretical cut-off size (x_{50})

For each centrifugation time at 1343 g, the increase in probability with increasing particle size for those smaller than x_{max} is observed (Figure 18). For those greater than x_{max}, the probability was reduced to 1.

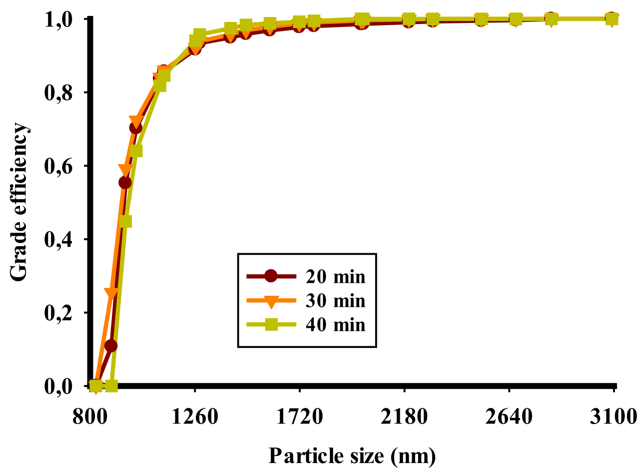

Figure 17. Variation in grade efficiency as a function of particle size for samples clarified at 1343 g.

Table 4. Estimated feed flow-rates for each commercial disk stack centrifuges.

Models	Σ Factor (m^2)	Operating time of the laboratory centrifuge (min)	Feed flow-rate of disc stack centrifuges (L/h)
Westfalia SAOOH	404.351	20	102.152
		30	68.101
		40	51.076
GEA OTC 2-03-107	204.469	20	51.655
		30	34.437
		40	25.828
SC6-06-076	857.071	20	216.523
		30	144.349
		40	108.262
Westfalia CSA-1	387.536	20	97.904
		30	65.269
		40	48.952
Frau CN2S	326.023	20	82.364
		30	54.909
		40	41.182
Culturefuge 100™	1666.380	20	420.980
		30	280.653
		40	210.490

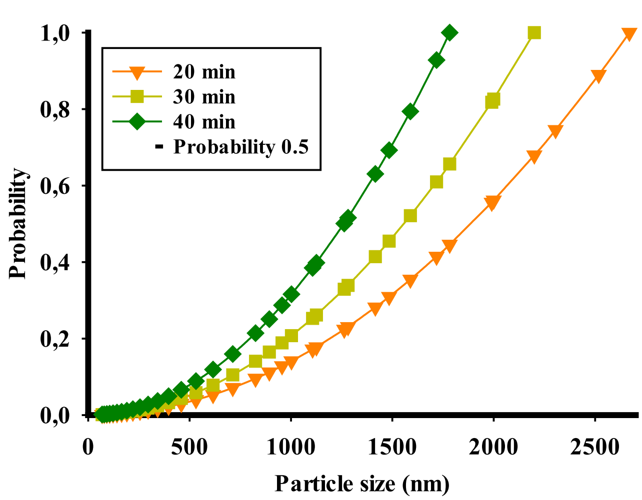

Figure 18. Probability as a function of particle size for continuous disc stack centrifuges.

This curve describes the probability for particles of a given particle size to be removed by centrifugation if the initial suspension consisted exclusively of them. This is the probability that could be obtained if the guava juice was clarified using a continuous disk stack centrifuge operating at 1343 g.

The cut-off size (x_{50}) corresponding to probability 0.5 was predicted. It varies for each treatment time; being 1887 nm, 1556 nm, 1261 nm, for 20 min, 30 min and 40 min, respectively. Increasing the centrifugation time would result in a decrease in the cut-off size. The decrease in surface area of particle size distribution curves with an increase in centrifugation time is accompanied by a decrease in the probability of particles of a specific size found in the supernatant after centrifugation.

4. Conclusion

In sum, the first objective of this paper was to determine the effect of centrifugal time and *g*-force on the physicochemical characteristics of clarified white-fleshed guava juice. The second objective was to identify the operational characteristics of a continuous centrifuge based on the performance of a fixed-angle conical rotor laboratory centrifuge. 97% w/w of clear guava juice could be recovered through centrifugation. Particle sizes of clear centrifuged juice samples ranged from 68 nm to 3100 nm compared to the feed sample with particle sizes comprised between 68 nm and 900,000 nm. 95.49% w/w of pectin and pectinaceous matters was removed during centrifugation with a decrease in dry matter content of 10.53% w/w. No significant change in physicochemical parameters and in the clarification efficiency of the fixed-angle conical rotor laboratory centrifuge used was observed for *g*-forces greater than 1343 g. With that acceleration, limits of separation or maximal particle sizes were determined and ranged from 1783 nm to 2669 nm for centrifugation times ranging from 20 to 40 min. Thanks to the clarification performance of the laboratory centrifuge, operational parameters of identified commercial disc stack centrifuges with given geometrical characteristics were determined. The predicted cut-off sizes ranged from 1261 nm to 1887 nm. Among these commercial centrifuges, Culturefuge 100™ model was the one with the highest predicted feed flow-rate.

Declarations

Author contribution statement

Kombele Aime Ninga: Conceived and designed the experiments; Performed the experiments; Analyzed and interpreted the data; Wrote the paper.

Steve Carly Zangue Desobgo; Emmanuel Jong Nso: Conceived and designed the experiments; Analyzed and interpreted the data; Contributed reagents, materials, analysis tools or data; Wrote the paper.

Joseph Kayem: Analyzed and interpreted the data.

Funding statement

This research did not receive any specific grant from funding agencies in the public, commercial, or not-for-profit sectors.

Data availability statement

Data included in article/supp. material/referenced in article.

Declaration of interests statement

The authors declare no conflict of interest.

Acknowledgments

The authors gratefully acknowledge the Departments of Process Engineering of the National School of Agro-Industrial Sciences (ENSAI), The

University of Ngaoundere (Cameroon) for providing necessary facilities for the successful completion of this research work.

Additional information

No additional information is available for this paper.

References

Akesowan, A., Choonhahirun, A., 2013. Effect of enzyme treatment on guava juice production using response surface methodology. J. Anim. Plant Sci. 23, 114–120.
Biswas, P.P., Mondal, M., De, S., 2016. Comparison between centrifugation and microfiltration as primary clarification of Bottle Gourd (Lagenaria siceraria) juice. J. Food Process. Preserv. 40, 226–238.
Boychyn, M., Yim, S.S., Bulmer, M., et al., 2004. Performance prediction of industrial centrifuges using scale-down models. Bioproc. Biosyst. Eng. 26, 385–391.
Cambiella, A., Benito, J.M., Pazos, C., Coca, J., 2006. Centrifugal Separation Efficiency in the Treatment of Waste Emulsified Oils. Chem. Eng. Res. Des. 84 (1), 69–76.
Chawafambira, A., StanleyT, N., Augustine, M., 2015. Production and optimisation of mango juice clarification using a manually pressurised filter at medium scale level in Rusitu valley, Zimbabwe. Int. J. Food Nutr. Sci. 4, 131–136.
Chhaya, Majumdar, G.C., De, S., 2013. Primary clarification of Stevia extract: a comparison between centrifugation and microfiltration. Separ. Sci. Technol. 48, 113–121.
Chlup, P.H., Bernard, D., Stewart, G.G., 2008. Disc Stack Centrifuge Operating Parameters and Their Impact on Yeast Physiology. J. Inst. Brew. 114 (1), 45–61.
Espuny, G., del, R.G., 2016. Scale-down characterisation of post-centrifuge flocculation processes and the study of its impact upon downstream processing during mammalian cell antibody production [The degree of. In: Doctor of Engineering]. University College, London.
Flores, G., Wu, S.B., Negrin, A., Kennelly, E.J., 2015. Chemical composition and antioxidant activity of seven cultivars of guava (Psidium guajava) fruits. Food Chem. 170, 327–335.
Ghosh, P., Pradhan, R.C., Mishra, S., 2018. Clarification of jamun juice by centrifugation and microfiltration: analysis of quality parameters, operating conditions, and resistance. J. Food Process. Eng. 41, e12603.
Malvern Instruments, 2013. Zetasizer Nano Series, User Manual. UK.
Jaarsveld, FP van, Blom, M., Hattingh, S., Marais, J., 2005. Effect of juice turbidity and yeast Lees content on brandy base wine and unmatured pot-still brandy quality. South Afr. J. Enol. Vitic. 26, 116–130.
Jain, A., De, S., 2016. Aqueous extraction of bitter gourd (Momordica charantia L.) juice and optimization of operating conditions. Fruits 71 (6), 379–387.
Jukkola, A., Hokkanen, S., Kämäräinen, T., Partanen, R., Heino, A., Rojas, O.J., 2019. Changes in milk fat globules and membrane lipids under the shear fields of microfiltration and centrifugation. J. Membr. Sci. 573, 218–225.
Kaur, S., Sarkar, B.C., Sharma, H.K., Singh, C., 2009. Optimization of enzymatic hydrolysis pretreatment conditions for enhanced juice recovery from guava fruit using response surface methodology. Food Bioprocess Technol. 2, 96–100.
Kaur, S., Sarkar, B.C., Sharma, H.K., Singh, C., 2011. Response surface optimization of conditions for the clarification of guava fruit juice using commercial enzyme. J. Food Process. Eng. 34, 1298–1318.
Koller, E., 2009. Sédimentation et décantation. In: Aide-mémoire Génie Chimique, 3e Edition. Dunod, L'usine Nouvelle, Paris, pp. 71–98.
Le, T.T., Nguyen, V.P.T., Le, V.V.M., 2012. Application of cellulase preparation to guava mash treatment in juice processing: optimization of treatment conditions by RSM. Asian J. Food Agro-Ind. 5, 284–291.
Marcelin, O., Smith, A.B., Bonnin, E., Brillouet, J.-M., 2017. Enzymatic breakdown of cell wall polysaccharides of guava (psidium GuajavaL.) puree. IOSR J. Environ. Sci. Toxicol. Food Technol. 11, 14–23.
Márquez-Montes, C.A., Gallegos-Infante, J.A., Rodrigo, G., et al., 2022. Centrifugal Cryoconcentration of Prickly Pear Juice: Effect on the Polyphenolic Content and Their Antioxidant Activity.
Maybury, J.P., Hoare, M., Dunnill, P., 2000. The use of laboratory centrifugation studies to predict performance of industrial machines: studies of shear-insensitive and shear-sensitive materials. Biotechnol. Bioeng. 67, 265–273.
McCready, R.M., McComb, E.A., 1952. Extraction and determination of total pectic materials in fruits. Anal. Chem. 24, 1986–1988.
McLellan, M.R., Padilla-Zakour, O.I., 2005. Juice processing. In: Barrett, D.M., Somogyi, L., Ramaswamy, H. (Eds.), Processing Fruits: Science and Technology, second ed. CRC Press, USA, pp. 73–96.
Nguyen, V.P.T., Le, T.T., Le, V.V.M., 2013. Application of combined ultrasound and cellulase preparation to guava (Psidium guajava) mash treatment in juice processing: optimization of biocatalytic conditions by response surface methodology. Int Food Res J 20, 377–381.
Ninga, K.A., Sengupta, S., Jain, A., et al., 2018. Kinetics of enzymatic hydrolysis of pectinaceous matter in guava juice. J. Food Eng. 221, 158–166.
Ninga, K.A., Desobgo, Z.S.C., De, S., Nso, J.E., 2021. Pectinase hydrolysis of guava pulp: effect on the physicochemical characteristics of its juice. Heliyon 7, e08141.
Nso, E.J., Ndibewu, P., Kayem, G.J., 1998. Reduction of viscosity of guava pulps by treatment with pectinases. Cameroon J. Biol. Biochem. Sci. 8, 7–16.
Omar, J.M., Nor, M.Z.M., Basri, M.S.M., Pa, C.N.F., 2020. Clarification of guava juice by an ultrafiltration process: analysis on the operating pressure, membrane fouling and juice qualities. Food Res. 4, 85–92.
Rai, P., De, S., 2009. Clarification of pectin-containing juice using ultrafiltration. Curr. Sci. 1361–1371.
Rayat, A.C., Chatel, A., Hoare, M., Lye, G.J., 2016. Ultra scale-down approaches to enhance the creation of bioprocesses at scale: impacts of process shear stress and early recovery stages. Curr. Opin. Chem. Eng. 14, 150–157.
Robatel, M., Borel, P., 1989. Centrifugation – Généralités, Théorie. In: Technique de l'Ingénieur, Traité Génie des Procédés. France, pp. 1–20.
Sagu, S.T., Nso, E.J., Karmakar, S., De, S., 2014. Optimisation of low temperature extraction of banana juice using commercial pectinase. Food Chem. 151, 182–190.
Sharma, H.P., Sharma, S., Prasad, K., 2015. Application of non thermal clarification in fruit juice processing-a review. South Asian J. Food Technol. Environ. 1, 15–21.
Shekhawat, L.K., Sarkar, J., Gupta, R., Hadpe, S., Rathore, A.S., 2018. Application of CFD in Bioprocessing: Separation of mammalian cells using disc stack centrifuge during production of biotherapeutics. J. Biotechnol. 267, 1–11.
Shomer, I., Yefremov, T., Merin, U., 1999. Involvement of proteins in cloud instability of Shamouti orange [Citrus sinensis (L.) Osbeck] juice. J. Agric. Food Chem. 47, 2623–2631.
Siebert, K.J., 1999. Protein - polyphenol haze in beverages. Food Technol.(Chicago) 53, 54–57.
Surajbhan, S., Alka, S., Chetan, J., Lambert, R., 2012. Extraction and optimization of guava juice by using response surface methodology. Am. J. Food Technol. 7, 326–339.
Svarovsky, L., 2000. Separation by centrifugal sedimentation. In: Solid – Liquid Separation, fourth ed. Butterworth – Heinemann, Oxford, pp. 246–280.
Towler, G., Sinnott, R., 2008. Equipment selection, specification, and design. In: Couldson and Richardson's Chemical Engineering, Chemical Engineering Design (Principles, Practice and Economics of Plant and Process Design). Butterworth-Heinemann, London, pp. 541–639.
Wu, J.S.-B., Wu, M.-W., Wei, Y.-P., 2005. Tropical fruits. In: Barrett, D.M.L.S., Ramaswamy, H. (Eds.), Processing Fruits: Science and Technology, second ed. CRC Press, USA, pp. 679–705.